Measurement of Single-Event Upsets in 65-nm SRAMs Under Irradiation of Spallation Neutrons at J-PARC MLF

Junya Kuroda, Seiya Manabe, Yukinobu Watanabe, Kojiro Ito, Wang Liao, Masanori Hashimoto, Shin-ichiro Abe, Masahide Harada, Kenichi Oikawa, and Yasuhiro Miyake

***Abstract*— A neutron irradiation test of static random access memories (SRAMs) was performed using a spallation neutron source at Materials and Life Science Experimental Facility (MLF) in the Japan Proton Accelerator Research Complex (J-PARC). The probability of neutron-induced single-event upsets (SEUs) was measured for 65-nm bulk and silicon on thin buried oxide (SOTB) SRAMs under neutron irradiation at the BL10 experimental facility. The measured SEU data were compared with the previous data of the same SRAMs which were measured at other irradiation facilities having different neutron spectra. The differences in the operating voltage dependence of the measured SEU probabilities are discussed with particular attention to the impact of irradiation side on SEUs. The particle and heavy ion transport code system (PHITS) simulation based on the simple sensitive volume model qualitatively reproduced the operating voltage dependence seen in the measured ratio of SEUs for the Bulk SRAM between the resin side and board side irradiations under different neutron fields.**

***Index Terms*— 65-nm bulk and silicon on thin buried oxide (SOTB) static random access memories (SRAMs), irradiation test, Japan Proton Accelerator Research Complex (J-PARC) Materials and Life Science Experimental Facility (MLF), neutron, particle and heavy ion transport code system (PHITS) simulation, single-event upset (SEU).**

Manuscript received December 23, 2019; revised February 21, 2020; accepted February 24, 2020. Date of publication March 4, 2020; date of current version July 16, 2020. This research was supported by Program on Open Innovation Platform with Enterprises, Research Institute and Academia, Japan Science and Technology Agency (JST, OPERA, JPMJOP1721).

Junya Kuroda, Seiya Manabe, and Yukinobu Watanabe are with the Department of Advanced Energy Engineering Science, Kyushu University, Fukuoka 816-8580, Japan (e-mail: kuroda.junya.114@s.kyushu-u.ac.jp; manabe@aees.kyushu-u.ac.jp; watanabe@aees.kyushu-u.ac.jp).

Kojiro Ito and Masanori Hashimoto are with the Department of Information Systems Engineering, Osaka University, Suita 565-0871, Japan (e-mail: i-kojiro@ist.osaka-u.ac.jp; hasimoto@ist.osaka-u.ac.jp).

Wang Liao was with the Department of Information System Engineering, Osaka University, Suita 565-0871, Japan. He is now with the School of Systems Engineering, Kochi University of Technology, Kami 782-8502, Japan (e-mail: liao.wang@kochi-tech.ac.jp).

Shin-ichiro Abe is with the Research Group for Radiation Transport Analysis, Japan Atomic Energy Agency (JAEA), Tokai 319-1195, Japan (e-mail: abe.shinichiro@jaea.go.jp).

Masahide Harada and Kenichi Oikawa are with the Materials and Life Science Division, J-PARC Center, Japan Atomic Energy Agency, Tokai 319-1195, Japan (e-mail: harada.masahide@jaea.go.jp; oikawa.kenichi@jaea.go.jp).

Yasuhiro Miyake is with the Muon Science Laboratory, High Energy Accelerator Research Organization (KEK), Tsukuba 319-1106, Japan, and also with the Materials and Life Science Division, Japan Proton Accelerator Research Complex Center, Muon Section, Tokai 319-1195, Japan (e-mail: ymiyake@post.kek.jp).

Color versions of one or more of the figures in this article are available online at http://ieeexplore.ieee.org.

Digital Object Identifier 10.1109/TNS.2020.2978257

I. Introduction

SOFT errors induced by terrestrial radiation in semiconductor devices have been of concern from the viewpoint of their reliability [1]–[3]. The soft error means a temporary malfunction in the devices due to single-event upsets (SEUs) caused by the transient signal induced by energetic ionizing radiation, e.g., resulting in upset of memory information in static random access memories (SRAMs). The SEU appears as a single-bit upset (SBU) or a multicell upset (MCU), where SBU and MCU mean the upset of one bit and of two or more bits, respectively, which are caused by a hit of a single particle or a photon. Until recently, the effect of cosmic-ray neutrons has been the main subject of a large number of investigations on radiation-induced soft errors at ground level [4]–[7]. Secondary ions such as alpha and heavy ions generated by neutron-induced reactions in very large-scale integrated (VLSI) chips cause the transient signal that results in SEUs. So far, we have conducted much research on cosmic-ray neutron-induced soft errors in modern complementary metal oxide semiconductor (CMOS) SRAMs and digital logic circuits, based on measurements and simulations. For instance, irradiation tests [8]–[10] were performed using a high-energy spallation neutron source at the Research Center for Nuclear Physics (RCNP), Osaka University [11] and a quasi-monoenergetic Li(p,n) neutron source at the Cyclotron and Radioisotope Center (CYRIC), Tohoku University [12].

Under these backgrounds, we have started a new irradiation experiment with spallation neutron beams at Materials and Life Science Experimental Facility (MLF) in the Japan Proton Accelerator Research Complex (J-PARC) [13] for the same SRAM devices as used in our previous irradiation tests. The two spallation neutron sources are now available in Japan, namely, RCNP and J-PARC MLF. As shown in Fig. 1, these experimental facilities can provide different neutron spectra. Since the previous data measured at RCNP and CYRIC are available for the same SRAMs, it is of much interest to investigate the sensitivity of neutron energy to SEUs by using the experimental data obtained by irradiation with different neutron spectra.

The purpose of the present work is to obtain SEU data for SRAM devices via irradiation of intensive spallation neutron beam available in the BL10 beam line at J-PARC MLF and then to compare it with the results from previous data obtained at CYRIC, while paying particular attention to the differences

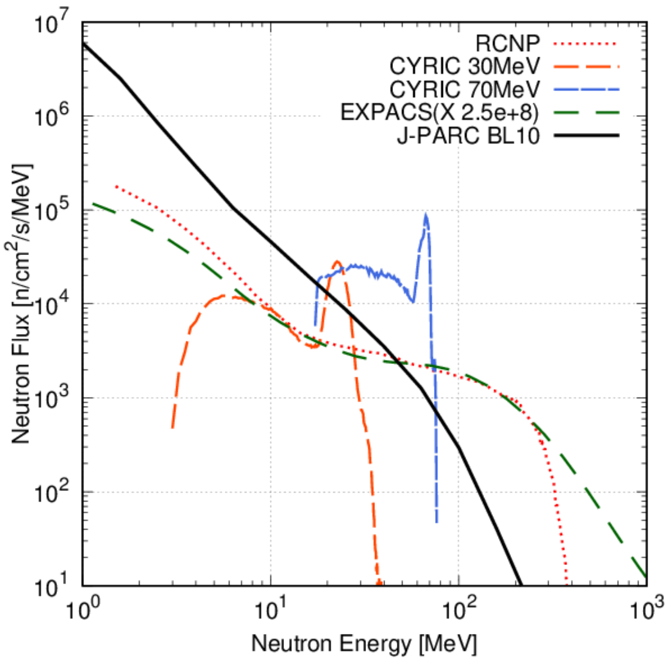

Fig. 1. Neutron spectra of experimental facilities (J-PARC BL10, RCNP, and CYRIC) and EXPACS calculation on the ground.

in cross sections from irradiating the resin side (RS) versus the board side (BS).

II. Experiment

A. Test Facility

The neutron irradiation test was performed using the BL10 beam line at J-PARC MLF. The facility produces neutrons through spallation reactions between incident 3-GeV protons and a mercury target [13], [14]. The pulsed neutrons cooled by a hydrogen moderator located above the target were formed into a square of 10 cm $\times$ 10 cm by a collimator and delivered to the BL10 irradiation room where a device under test (DUT) was placed. The energy spectrum of incident neutrons was derived using the simulation result [14] with the number of incident 3-GeV protons that was calculated from the average beam current monitored during each irradiation test. Table I presents the fraction of neutrons in three energy groups for BL10, RCNP, and cosmic-ray neutrons on the ground calculated by Excel-based Program for calculating Atmospheric Cosmic-ray Spectrum (EXPACS) [15]. As shown in Fig. 1 and Table I, the J-PARC BL10 neutron field has a characteristic neutron spectrum having a much higher proportion of low-energy neutrons than the other neutron fields. The neutron flux at J-PARC BL10 contains thermal component in a normal operation mode. In the present irradiation test, a 1-cm-thick sintered boron carbide (B_4C) plate was installed at 7.1-m position of the beam line to absorb the thermal neutrons.

B. Experimental Setup

The experimental setup is shown in Fig. 2. The two DUTs were placed at 13.4 and 14 m from the hydrogen moderator.

TABLE I

Fraction of Neutrons Included in Each Energy Group in the J-PARC BL10 and RCNP Facilities, and the Neutron Spectrum on the Ground Calculated by EXPACS [15]

Energy domain	BL10[%]	RCNP[%]	EXPACS[%]
1-10MeV	91.7	52.0	36.4
10-100MeV	8.0	27.8	31.0
>100MeV	0.2	20.2	32.6

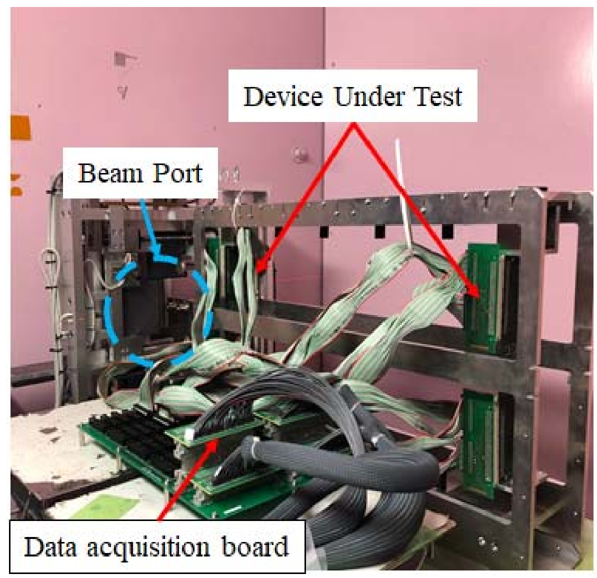

Fig. 2. Experimental setup.

Both DUTs were connected to a large-scale integration (LSI) tester to count the number of SEUs via the data acquisition board.

Fig. 3 shows the structure of the DUT. Bulk and silicon on thin buried oxide (SOTB) SRAM chips fabricated in a 65-nm CMOS technology with a deep-well option were used in the experiment. Each of chips contains 12-Mbit memory cells of 6T design. In the chips, 64 BL $\times$ 2 WL cells share the same well [9]. The 16 SRAM chips are mounted on a piece of printed circuit board (PCB) and are covered by epoxy resin. Note that the same DUTs were tested at RCNP and CYRIC in the previous work [9], [10].

The neutron beam irradiated each test board from one side at a time. As shown in Fig. 3, one was from the "RS" and the other from the "BS" to confirm the impact of irradiation side on the occurrence of SEU which was discussed in [10]. Additionally, the operating supply voltage of SRAMs was changed in each irradiation run to investigate the voltage dependence of the SEU rate.

III. Results and Discussion

A. Operating Voltage Dependence of SEUs

Fig. 4 shows the operating voltage dependence of the SEUs occurrence probability (P_{SEU}) measured for the Bulk SRAM at J-PARC BL10 under neutron irradiation from the RS and the

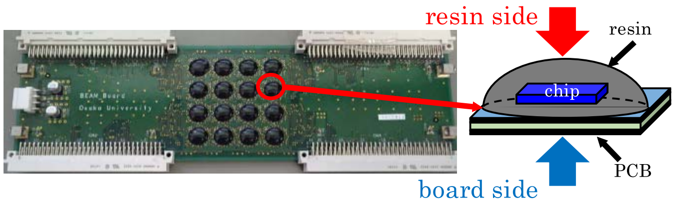

Fig. 3. DUT used in the experiment.

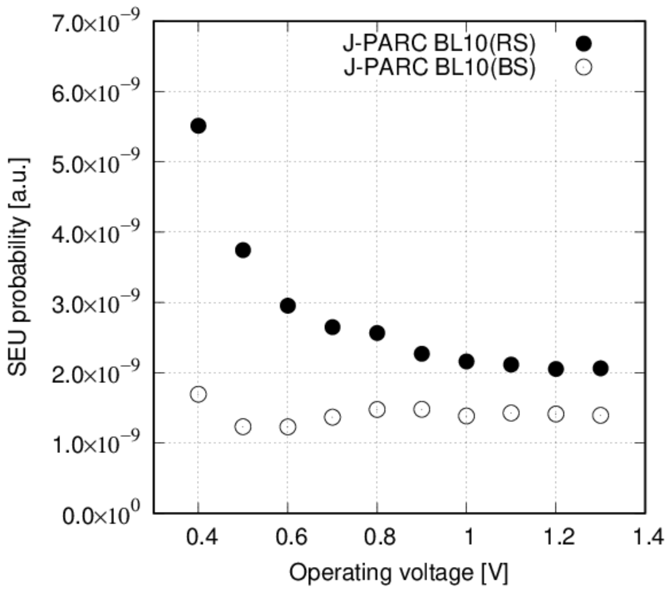

Fig. 4. Voltage dependence of the SEU probability measured for the Bulk SRAM at J-PARC BL10. Each statistical error is within the symbol. The unit (a.u.) of the vertical axis means arbitrary unit.

BS. The probability P_{SEU} was defined by the number of upset bits per incident neutron fluence. First, we found that there is a large difference in P_{SEU} between RS and BS irradiations and the former P_{SEU} is larger than the latter P_{SEU} across the entire operating voltage range. In the case of RS irradiation, P_{SEU} monotonically decreases with an increase in the operating voltage. On the other hand, the P_{SEU} observed under the BS irradiation reaches a minimum value at the operating voltage between 0.5 and 0.6 V, and increases to a saturated value above 0.6 V. As discussed in [9], we expect that this tendency observed in the BS irradiation data appears due to the balance of the following two effects. The critical charge increases as the operating voltage reduces. In this case, P_{SEU} increases with a decrease in the operating voltage. On the other hand, the contribution of parasitic bipolar effect (PBE) to P_{SEU} increases as the operating voltage rises. By balancing the two effects, it can be explained that P_{SEU} has a minimum point.

The experiment at CYRIC was performed under irradiation from both sides (RS and BS) of the DUT in the same way as in the present work. Fig. 5 presents the voltage dependence of P_{SEU} for the Bulk SRAM measured at CYRIC [9]. The same tendency of P_{SEU} as under the BS irradiation (see Fig. 4) is observed. The P_{SEU} under the RS irradiation is larger than that under the BS irradiation at any of three operating voltages of 0.5, 0.9, and 1.2 V. This is the same as in the J-PARC

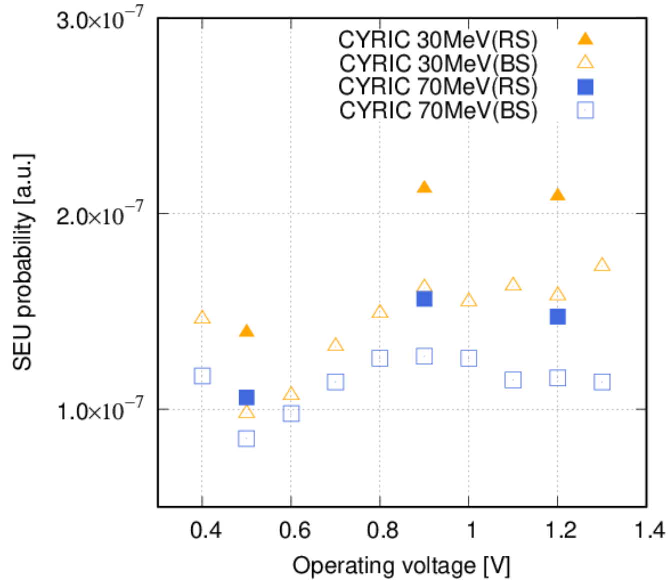

Fig. 5. Voltage dependence of the SEU probability measured for the Bulk SRAM at CYRIC. The experimental data are taken from [9].

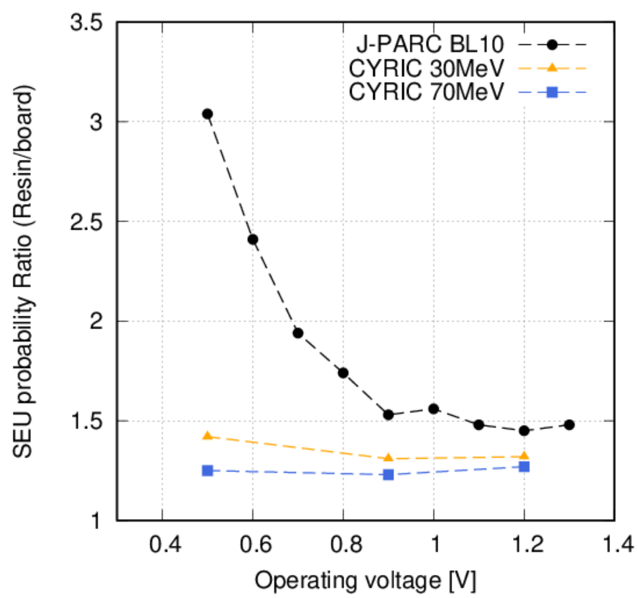

Fig. 6. Ratio of the SEU probability under the RS Irradiation against BS irradiation for the Bulk SRAM.

BL10 data shown in Fig. 4. From comparison of Figs. 4 and 5, the tendency observed under the RS irradiation at J-PARC BL10 is found to be different from the experimental results of the other irradiation conditions, i.e., monotonic decrease trend with an increase in the operating voltage. The analysis and discussion with attention to hydrogen included in the epoxy resin is presented for understanding of this characteristic tendency in Section III-C.

Fig. 6 shows the ratio of P_{SEU} under the RS irradiation to P_{SEU} under the BS irradiation measured in three different neutron fields. The ratio of P_{SEU} measured at CYRIC is smaller than that measured at J-PARC BL10, especially at

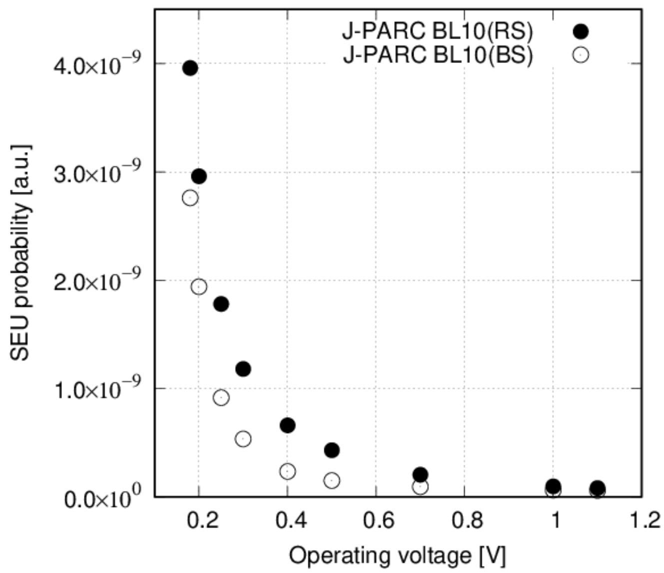

Fig. 7. Voltage dependence of the SEU probability measured for the SOTB SRAM at J-PARC BL10. Each statistical error is within the symbol.

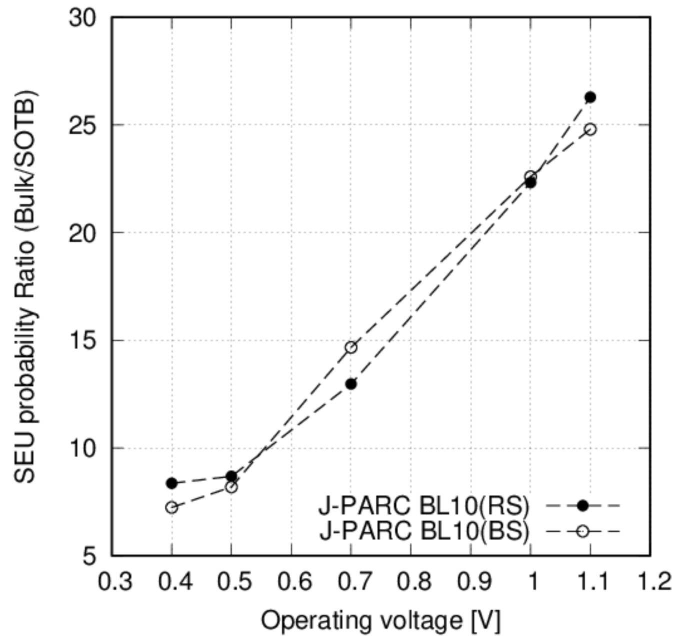

Fig. 8. Ratio of the SEU probability between the Bulk and SOTB SRAMs measured at J-PARC BL10.

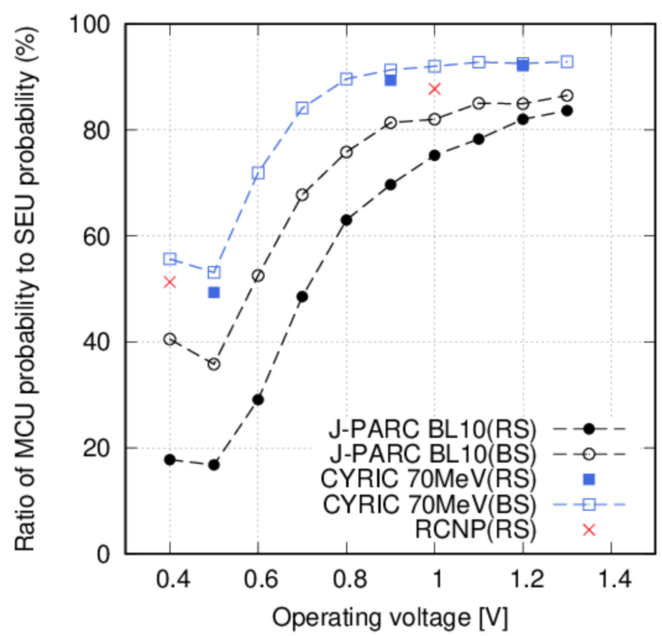

Fig. 9. Ratio of the MCU probability to the SEU probability of the Bulk SRAM.

low operating voltage. Finally, we found that P_{SEU} under the RS irradiation is larger than P_{SEU} under the BS irradiation, regardless of operating voltage, in either case of neutron irradiations with J-PARC BL10 and CYRIC.

In Fig. 7, the voltage dependence of the measured P_{SEU} of the SOTB SRAM is compared between the RS and BS irradiations at J-PARC BL10. The probability P_{SEU} was defined by the number of upset bits per incident neutron fluence. The experimental result shows a similar voltage dependence of the SEU probability, regardless of the irradiation side, which is different from the result of the Bulk SRAM seen in Fig. 4.

Fig. 8 shows the ratio of P_{SEU} of the Bulk SRAM to that of the SOTB SRAM measured at J-PARC BL10. The ratio increases with operating voltage. This indicates that the SOTB SRAM has higher tolerance characteristics than the Bulk SRAM across the entire range of operating voltage. As will be discussed in Section III-B, the tendency may be due to much smaller occurrence probability of MCUs in the SOTB SRAM than that in the Bulk SRAM.

B. Operating Voltage Dependence of MCUs

We compare the MCUs measured at J-PARC BL10, CYRIC, and RCNP. Fig. 9 shows the ratio of the MCU probability (P_{MCU}) to the SEU probability (P_{SEU}) as a function of operating voltage. For the CYRIC data, only the data with 70-MeV irradiation are given in Fig. 9, because there is no observable difference between 30- and 70-MeV irradiations. The RCNP data are given for RS irradiation at the two operating voltage of 0.4 and 1.0 V, which are close to the CYRIC data.

First, the ratio has a minimum at the operating voltage of 0.5 V and gradually increases above 0.5 V, regardless of different neutron fields and irradiation sides. Liao *et al.* [16] indicated that the PBE is likely to lead to a significant increase in MCUs as the operating voltage rises. From their discussion, the behavior of the ratio in Fig. 9 seems to be caused by the PBE. As shown in Fig. 4, no dip was observed at 0.5 V in the P_{SEU} measured under the RS irradiation at J-PARC BL10, while the P_{MCU} has the minimum value at 0.5 V under the same irradiation condition in Fig. 9.

Next, we compare the SBUs and MCUs observed in the J-PARC BL10 and CYRIC experiments. In Fig. 10, the ratios of the total bit numbers of SBU and MCU between the RS and BS irradiations are plotted as a function of operating voltage. The ratios for the CYRIC experiment are almost

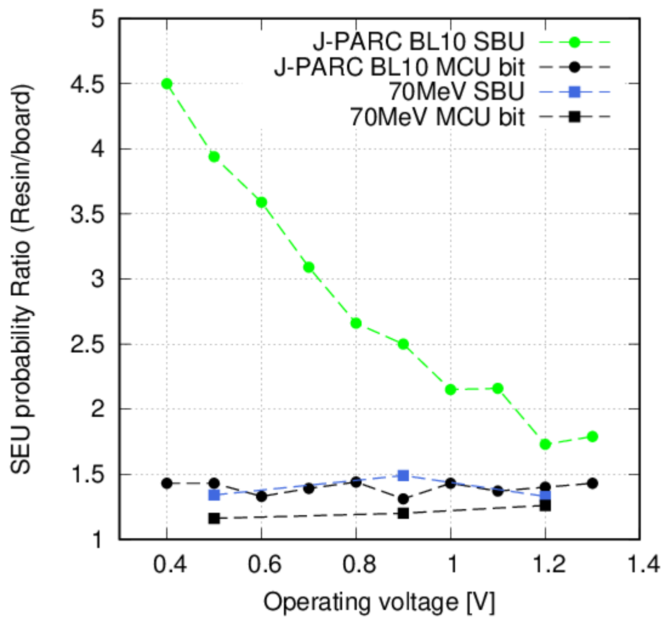

Fig. 10. Ratio of the SBU and MCU probabilities of the Bulk SRAM between the RS and BS irradiations.

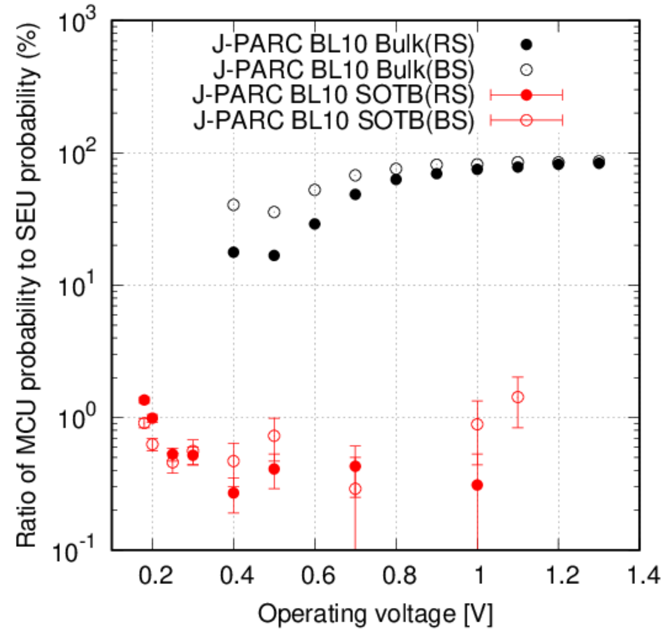

Fig. 11. Ratios of the MCU probability to the SEU probability for the Bulk and SOTB SRAMs. The error bar represents one standard deviation.

constant regardless of the operating supply voltage. The MCU ratio observed in the J-PARC BL10 experiment shows the same tendency as in the CYRIC experiment. However, one can see that the SBU ratio for the J-PARC BL10 experiment remarkably increases with a decrease in operating voltage and is larger than the other ones in a whole range of the operating voltage. This result suggests that the difference of P_{SEU} between the irradiation sides observed in the J-PARC BL10 experiment seen in Fig. 4 arises from the difference in the fraction of SBU in SEUs. As shown in Fig. 1 and Table I, the J-PARC BL10 neutron spectrum has a large fraction of low-energy neutrons below 10 MeV. We presume that the low-energy neutrons caused SBU more frequently than MCU. To understand this, we have performed a simulation based on a simple model and the result will be discussed in Section III-C.

Finally, the ratios of P_{MCU} to P_{SEU} are compared between the Bulk and SOTB SRAMs in Fig. 11. The closed and open symbols represent the irradiations from RS and BS, respectively. From the comparison, it was found that the percentage of MCUs observed in the SOTB SRAM is less a few % and much smaller than that in the Bulk SRAM. We expect that this large difference in MCU occurrence between both SRAM devices leads to high soft error resistance for SOTB devices.

C. Monte Carlo Simulation

A Monte Carlo (MC) simulation with particle and heavy ion transport code system (PHITS) [17] was performed for estimating the deposited charge in the Bulk SRAM cell. The SRAM structure and the experimental conditions including the neutron spectrum were considered properly in the PHITS simulation according to our previous work [9]. We defined the sensitive volume (SV) including the depletion region and calculated the charge deposited in the SV by secondary ions generated via neutron-induced reactions with the constituent material. The number of SEUs per neutron is assumed to be the number of the events in which the charge deposited in SV exceeds a defined critical charge, Q_c.

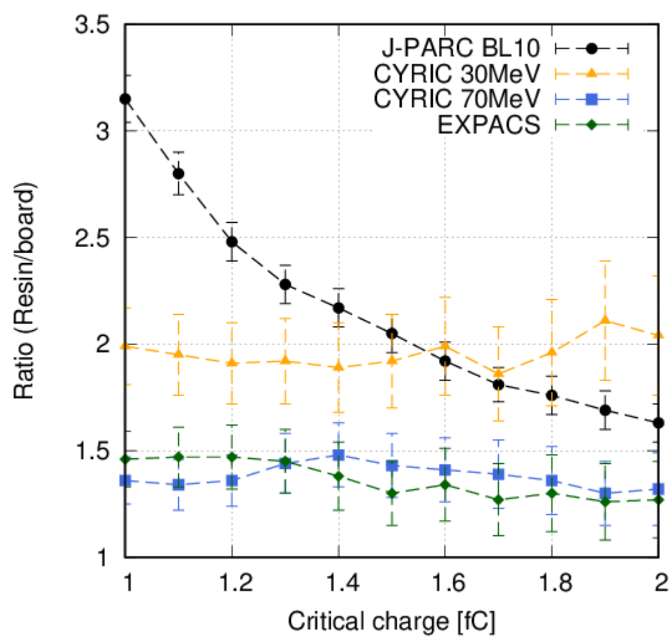

Fig. 12. Ratio of the SEUs in the Bulk SRAM simulated by PHITS for the RS irradiation to those for the BS irradiation.

Fig. 12 shows the calculated ratio of SEUs for RS and BS irradiations under four different neutron fields as a function of critical charge. The error bars represent the statistical uncertainties in the MC calculation. This simulation result can be compared with the experimental result shown in Fig. 6. The low critical charge corresponds to the low operating voltage.

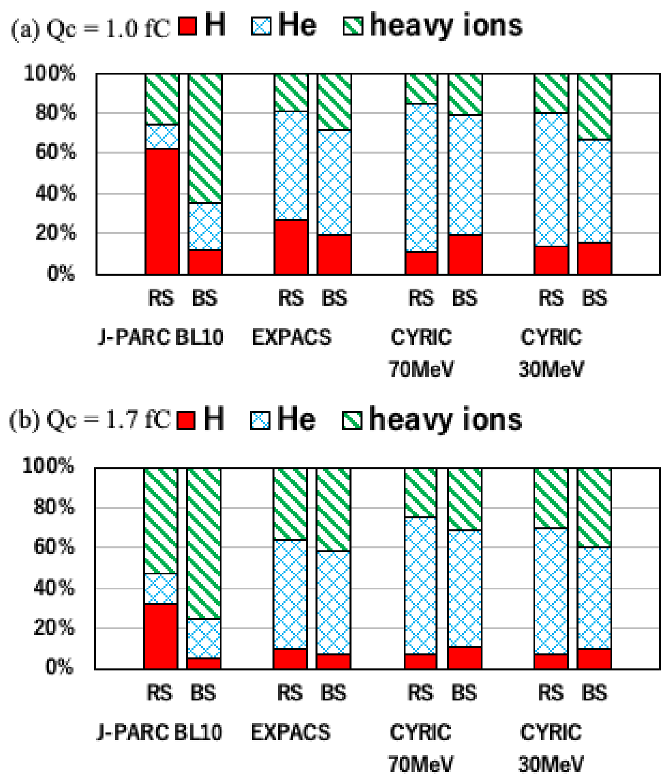

Fig. 13. Relative contribution of individual secondary ions to the simulated SEUs in the case of the Bulk SRAMs with (a) $Q_c = 1.0$ fC and (b) 1.7 fC for two irradiation sides, i.e., the RS and the BS.

The experimental ratio is reproduced by the simulation qualitatively well. In particular, the simulation satisfactorily reproduces the increasing trend in the experimental ratio seen in the low-operating-voltage domain for the J-PARC BL10 irradiation test. The EXPACS result simulating the terrestrial environmental neutron spectrum shows the small ratio of the SEU probability. As can be seen in Fig. 12, the dependence of irradiation sides on SEUs becomes weak under irradiation in the neutron fields with high-energy components.

The J-PARC BL10 irradiation field has a large amount of low-energy neutrons below 10 MeV compared to the 30- and 70-MeV quasi-monoenergetic neutron fields. Abe *et al.* [10] discussed the impact of irradiation side on the SEUs by the 30- and 70-MeV quasi-monoenergetic neutrons. They revealed that the existence of hydrides in the resin considerably increases the SEUs because of higher production yields of secondary hydrogen (H) ions, namely, protons that are generated via neutron elastic scattering with hydrogen atoms. The neutron–proton (n–p) elastic scattering cross section increases as the incident neutron energy decreases. In addition, the recoiled proton is emitted to only forward angle in the case of the n–p scattering, resulting in high probability for the recoiled proton to pass through the SV. Moreover, we found that the fraction of SBU in SEU is much larger at low operating voltage as shown in Fig. 9. Since the proton has smaller linear energy transfer (LET) than heavier ions such as He and Si ions, we expect that SBUs are more predominant than MCUs in the SEUs caused by recoiled protons.

To confirm the effect of the recoiled proton, we show the relative contribution of individual secondary ions (proton, alpha particle, and other heavy ions) to the simulated SEU probability of the Bulk SRAM in Fig. 13. The results of $Q_c = 1.0$ and 1.7 fC are given in the upper and lower figures of Fig. 13, respectively. The simulation with the J-PARC BL10 neutron spectrum indicates the larger contribution of protons in the RS irradiation compared to the BS irradiation, because the resin contains more hydrogen. In addition, we found that the relative contribution of proton is reduced in the simulation with $Q_c = 1.7$ fC, because the LET of protons is less than that of the other ions and the events that the charge deposited in the SV exceed Q_c decreases. Note that the secondary proton is mainly generated by the (n,p) reaction on Si in the BS irradiation. The simulation results with the CYRIC and EXPACS neutron spectra show that there is no large difference in the relative contribution of protons between the RS and BS irradiations.

From the PHITS simulation with the simple SV model, thus, we have found that the large ratio of the SEU probability of the Bulk SRAM under the RS irradiation to that under the BS irradiation observed at J-PARC BL10 is due mainly to the recoiled protons that are generated via elastic scattering of low-energy neutrons with hydrogen atoms in the resin.

IV. Conclusion

We took the SEU data for 65-nm Bulk and SOTB SRAMs under irradiation of spallation neutrons at the BL10 beam line in J-PARC MLF.

The experimental SEU data of the Bulk SRAM were compared with the previous data of the same SRAMs measured at the other neutron facilities with different neutron spectra, RCNP and CYRIC. One of the differences in the SEUs among them is the operating voltage dependence of the SEU probability. We found that the SEU probability under the BS irradiation for the Bulk SRAM has the monotonic decrease trend with an increase in the operating voltage in the J-PARC BL10 data. The measured SEUs were decomposed into two components, SBU and MCU, to investigate what causes the difference. The fraction of MCU in the SEUs measured at the J-PARC BL10 neutron field was found to be lower than those measured at RCNP and CYRIC. In addition, we found that the MCU probability has no large difference between the RS irradiation and the BS irradiation, while the SBU probability is large in the RS irradiation compared to the BS irradiation.

The experimental SEU data of the SOTB SRAM were compared with those of the Bulk SRAM. The SOTB SRAM showed higher tolerance characteristics than the Bulk SRAM over the entire range of operating voltage. The higher tolerance can be explained by the small MCU probability of the SOTB SRAM than that of the Bulk SRAM, especially at high operating voltage.

The PHITS simulation with the simple SV model qualitatively reproduces the experimental ratio of SEUs for RS and BS irradiations on the Bulk SRAM in three different neutron fields. From the present simulation and the previous work [4], the large ratio observed in the J-PARC BL10 data at low operating voltage can be explained by the influence of the protons generated by neutron elastic scattering with hydrogen atoms in the resin. In the future, we plan to perform more detailed analysis of the experimental results based on the PHITS simulation with the multi-SV model used in [4].

Acknowledgment

This neutron experiment was at the Materials and Life Science Experimental Facility of the J-PARC under a user program No. 2018B0021.

References

[1] R. Silberberg, C. H. Tsao, and J. R. Letaw, "Neutron generated single-event upsets in the atmosphere," *IEEE Trans. Nucl. Sci.*, vol. NS-31, no. 6, pp. 1183–1185, Dec. 1984.

[2] D. Thouvenot, P. Trochet, R. Gaillard, and F. Desnoyers, "Neutron single event effect test results for various SRAM memories," in *Proc. IEEE Radiat. Effects Data Workshop NSREC Snowmass. Workshop Rec. Held Conjunct IEEE Nucl. Space Radiat. Effects Conf.*, Jul. 1997, pp. 61–66.

[3] M. Ohlsson, P. Dyreklev, K. Johansson, and P. Alfke, "Neutron single event upsets in SRAM-based FPGAs," in *Proc. IEEE Radiat. Effects Data Workshop. NSREC, Workshop/IEEE Nucl. Space Radiat. Effects Conf.*, Jul. 1998, pp. 177–180.

[4] Y. Yahagi *et al.*, "Versatility of SEU function and its derivation from the irradiation tests with well-defined white neutron beams," *IEEE Trans. Nucl. Sci.*, vol. 52, no. 5, pp. 1562–1567, Oct. 2005.

[5] M. S. Gordon *et al.*, "Measurement of the flux and energy spectrum of cosmic-ray induced neutrons on the ground," *IEEE Trans. Nucl. Sci.*, vol. 51, no. 6, pp. 3427–3434, Dec. 2004.

[6] T. Nakamura, E. Ibe, M. Baba, Y. Yahagi, and H. Kameyama, *Terrestrial Neutron Induced Soft Error in Advanced Memory Devices*. Singapore: World Scientific, 2008.

[7] E. H. Ibe, *Terrestrial Radiation Effects in ULSI Devices and Electronic Systems*. Hoboken, NJ, USA: Wiley, 2015.

[8] S. Hirokawa, R. Harada, K. Sakuta, Y. Watanabe, and M. Hashimoto, "Multiple sensitive volume based soft error rate estimation with machine learning," in *Proc. 17th Eur. Conf. Radiat. Effects Compon. Syst. (RADECS)*, Sep. 2016, Paper H17.

[9] W. Liao, M. Hashimoto, S. Manabe, S.-I. Abe, and Y. Watanabe, "Similarity analysis on neutron- and negative muon-induced MCUs in 65-nm bulk SRAM," *IEEE Trans. Nucl. Sci.*, vol. 66, no. 7, pp. 1390–1397, Jul. 2019, doi: 10.1109/TNS.2019.2921365.

[10] S. Abe, W. Liao, S. Manabe, T. Sato, M. Hashimoto, and Y. Watanabe, "Impact of irradiation side on neutron-induced single-event upsets in 65-nm bulk SRAMs," *IEEE Trans. Nucl. Sci.*, vol. 66, no. 7, pp. 1374–1380, Jul. 2019, doi: 10.1109/TNS.2019.2902176.

[11] Y. Iwamoto *et al.*, "Evaluation of the white neutron beam spectrum for single-event effects testing at the RCNP cyclotron facility," *Nucl. Technol.*, vol. 173, no. 2, pp. 210–217, Apr. 2017.

[12] Y. Sakemi, M. Itoh, and T. Wakui, "High intensity fast neutron beam facility at CYRIC," *Int. Atom. Energy Agency*, vol. 46, no. 9, pp. 229–233, 2014.

[13] F. Maekawa *et al.*, "NOBORU: J-PARC BL10 for facility diagnostics and its possible extension to innovative instruments," *Nucl. Instrum. Methods Phys. Res. A, Accel. Spectrom. Detect. Assoc. Equip.*, vol. 600, no. 1, pp. 335–337, Feb. 2009.

[14] M. Harada, F. Maekawa, K. Oikawa, S.-I. Meigo, H. Takada, and M. Futakawa, "Application and validation of particle transport code PHITS in design of J-PARC 1 MW spallation neutron source," *Progr. Nucl. Sci. Technol.*, vol. 2, no. 0, pp. 872–878, Oct. 2011.

[15] T. Sato. *EXPACS 2009*. Accessed: Dec. 19, 2019. [Online]. Available: http://phits.jaea.go.jp/expacs/jpn.html

[16] W. Liao *et al.*, "Measurement and mechanism investigation of negative and positive muon-induced upsets in 65-nm bulk SRAMs," *IEEE Trans. Nucl. Sci.*, vol. 65, no. 8, pp. 1734–1741, Aug. 2018.

[17] T. Sato *et al.*, "Features of particle and heavy ion transport code system (PHITS) version 3.02," *J. Nucl. Sci. Technol.*, vol. 55, no. 6, pp. 684–690, Jan. 2018.